TERRAIN SURFACE RECONSTRUCTION
BY THE USE OF TETRAHEDRON MODEL WITH THE MDL CRITERION

G. Sohn, I. Dowman

Dept. of Geomatic Engineering, University College London, Gower Street, London, WC1E 6BT UK – (gsohn, idowman)@ge.ucl.ac.uk

Commission III, WG III/3

KEY WORDS: LIDAR, Automation, DEM/DTM, Filtering

ABSTRACT:

A LIDAR filtering technique is used to differentiate on-terrain points and off-terrain points from a cloud of 3-D point data collected by a LIDAR system. A major issue of concern in this low-level filter is to design a methodology to have a continual adaptation to terrain surface variations. To this end, several essential observations are discussed in this paper: i) the terrain surface can be fragmented into a set of piecewise "homogeneous" plane surfaces, in which terrain surface variations are smoothed out, ii) a criterion for differentiating on- and off-terrain point from plane terrain surface can be equivalently applied to these terrain segments assumed as being plane, and iii) an inter- and intra-relationship of on- and off-terrain points can be as verifying the *a priori* taken assumption of the plane terrain surface. The main strategy implemented in our LIDAR filtering technique is to iteratively generate a number of terrain surface models in order to hypothesize and test a plane terrain surface over a local area. Finally, the most reliable plane terrain surface model is selected as an optimised solution and thus the terrain surface model is refined. To this end, we devise a two-step *divide-and-conquer* triangulation in terms of downward and upward model refinement; in this framework, a tetrahedron is used in order to hypothesize a plane terrain surface and the *Minimum Description Length* (MDL) criterion is employed for the selection of an optimized plane terrain surface model. The useful characteristics of this method are discussed with results derived from real LIDAR data.

1. INTRODUCTION

Recently, LIDAR technology has been getting much more attention from the photogrammetry, remote sensing, surveying and mapping community as an important new data source for a wide range of applications; topographic mapping, bathymetry, forest mapping, crop height measurement, flood modelling and 3-D building modelling (Cobby et al., 2001). Among the many algorithmic methodologies used to generate the above value-added products, a filtering technique to differentiate on-terrain points from off-terrain points has been emphasized as an efficient focusing strategy to understand complex scenes. Although various types of filtering techniques have been introduced (Pfeifer & Kraus, 1998; Axelsson, 2000; Vosselman, 2000), Flood (2001) reported that 60% - 80% of LIDAR data processing lines running in private firms is allocated to manual classification and final quality control, due to the lack of efficient algorithms for extracting the bare earth surface.

2. PROBLEM DESCRIPTION

2.1 Labelling Problem

A LIDAR filtering technique to differentiate on- and off-terrain points from a point cloud can be considered as a low-level vision problem. Such a low-level filtering technique is often posed as a labelling problem in which predefined semantic labels are assigned to data (Li, 2001).

Suppose that we have a set of discrete LIDAR points S and a labelling function F which assigns pre-designed semantic labels, namely {on, off} to the data domain S. The labelling function F generates a set of new labelling observations f, which can be described as follows:

$$
\begin{aligned}
S &= \{s_i\}_{i=1}^{N} \\
f &= \{f_i\}_{i=1}^{N};\ f_i = \mathrm{F}(s_i);\ f_i \in \{on, off\}
\end{aligned}
\tag{1}
$$

where i is the index of discrete point s; N is the dimension of the domain S; f_i is a label assigned to the point s_i from a label set {on, off}.

In order to give the labelling function F of Eq. (1) an actual method to populate wanted terrain labels, a criterion δ to differentiate on- and off-terrain points is needed. A major issue concerned in the selection of δ is how to make δ robust under the circumstances where background knowledge about underlying terrain slope has changed; when terrain slope changes gently or abruptly. This scale issue governs the overall performance of the filter. Figure 1 illustrates a simple example where a criterion δ is selected to differentiate on- and off-terrain points from a flat terrain surface; a point with slope angle larger than δ is labelled as an off-terrain point; otherwise, it is labelled as an on-terrain point (see Figure 1(a)). However, when a point is located in a different background, this criterion δ is not valid any more since the background knowledge that the terrain surface is flat has been altered (see Figure 1(b)).

There may be two ways to tackle this problem. One is to make δ adaptive to underlying terrain slope; δ is trained with the analysis of background knowledge about terrain slope collected

within pre-specified areas (Vosselman, 2000); a statistic median value of slope angle distribution characterize a terrain slope of an investigated local area (Axelsson, 2000); a "good" mixture of on- and off-terrain points over a local area is assumed so that it facilitates an iterative terrain resampling process as its parameters of weighting function are implicitly determined (Pfeifer&Kraus, 1998).

In contrast to this, the other method devised in our current work is to fragment the entire terrain surface into a set of piecewise segments so that they have "homogeneous" background knowledge of the underlying terrain slope as being "plane". In this context, a criterion δ is explicitly selected in such a way as to differentiate on- and off-terrain point from a "plane" terrain. This can be universally applied to overall terrain segments regardless of terrain surface variances since all terrain segments are assumed to be plane terrain surfaces. Hence, a LIDAR filtering technique could be converted into a problem to look for a set of plane terrain surfaces into which terrain surface variation is regularized, rather than to estimate δ itself.

To achieve this goal, it is necessary to use a terrain surface model ψ to hypothesize a set of plane terrain surfaces, and a criterion δ that is independent of the model ψ. In this approach, the labelling problem in Eq. (1) can be rewritten as follows:

$$f = \{f_i\}_{i=1}^{N};\ f_i = F(s_i \mid \psi, \delta);\ f_i \in \{on, off\} \tag{2}$$

where a label f_i for LIDAR point s_i is determined when a terrain surface model ψ and a criterion δ are given.

(a) δ applied on a flat terrain surface

(b) δ applied on a terrain surface with the mixture of variousterrain scales
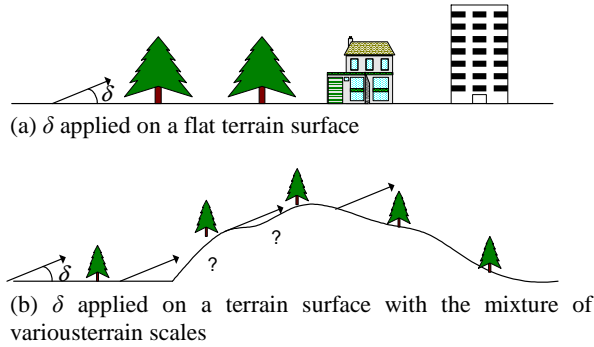
Figure 1. Illustration of terrain scale dependency of δ when given δ is explicitly applied on various types of terrain scales as a slope angle criterion.

2.2 Terrain Surface Reconstruction Problem

Suppose then our terrain surface model ψ in Eq. (2) can be described as a set of piecewise planar surface models $\{\phi_j\}$ as follows:

$$\psi = \{\phi_j\}_{j=1}^{M};\ \phi_j = \begin{bmatrix} a_j & b_j & c_j \end{bmatrix};\ \phi_j \mathbf{s}_j^{on} = 0 \tag{3}$$

where j is the model index of the piecewise planar surface model ϕ; $\begin{bmatrix} a_j & b_j & c_j \end{bmatrix}$ is the parameter vector of the planar model ϕ_j; $\mathbf{s}_j^{on}$ is the vector of the LIDAR point s_j located within ϕ_j, which is labelled as on-terrain point when the labelling function F is given; $F(s_j \mid \phi_j, \delta) = \{on\}$. In Eq. (3), the planar terrain surface model ϕ_j is made of the on-terrain points only, which is satisfied with the condition $\phi_j \mathbf{s}_j^{on} = 0$ and M is the dimension of the model space ψ created when the entire domain S is initialised as the on-terrain point, $F(S) = \{on\}$.

Now, a terrain surface reconstruction problem can be reformulated to determine a global optimised solution ψ^*, which is obtainable from the searching process of a local optimised solution ϕ_j^* as follows:

$$\psi^*\left(\phi^*, k\right) = \{\phi_j^*\}_{j=1}^{k};\ \phi_j^*\left(\mathbf{s}_j^*\right)^{on} = 0 \tag{4}$$

where ϕ_j^* is the locally optimised piecewise planar surface model; k is the dimension of the model space ψ^*, which is less than M of Eq. (3); $\left(\mathbf{s}_j^*\right)^{on}$ is the vector of on-terrain points located within ϕ_j^*. Eq. (4) presents us with several important points to be noted in reconstructing the terrain surface.

- It considers the dimension k of an optimal terrain surface model ψ^* as a variable to be determined during a terrain surface model reconstruction process, rather than being a pre-fixed constant as in Baillard & Maitre's work (1999), in which global labelling observations are optimized within a pre-specified number of flat terrain models having almost the same size.

- A locally determined planar surface model ϕ_j^* is required to be comprised of on-terrain points. Thus, the determination of k is directly related to the number of on-terrain points found, where k increases as on-terrain points are iteratively obtained.

- The methodology to achieve an optimal solution ψ^* shown in Eq. (4) is based upon a local optimisation approach rather than a global minimisation technique. That is, a planar surface model is found as a local optimal solution ϕ_j^* and thus the global terrain surface model ψ^* is determined as a set of local optimal solutions $\{\phi^*\}$.

It is necessary to discuss an optimality criterion of ϕ_j^* used in Eq. (4). In Eq. (2), the labelling observation f of the LIDAR points S is determined using a criterion δ under the assumption that underlying terrain surface is "correctly" reconstructed as flat by a planar surface model. However, if its assumption is not valid, the labelling error of f becomes large so that real on-terrain points are misclassified into off-terrain and vice versa. Thus, the optimality is achieved when labelling observation f generated supports most properly the prescribed assumption of plane terrain surface.

To obtain these local optima, we adopt the hypothesis-test approach. A local terrain is hypothesized as a plane terrain surface by a number of planar surface model candidates $\{\phi_j^c\}$. According to Eq. (2), corresponding labelling observations $\{f_j^c\}$ can be generated when δ is given. We can then try to measure the closeness between a model candidate ϕ_j^c and its observation f_j^c to test the hypothesis of a plane terrain surface reconstructed by ϕ_j^c. Such closeness measurement can be described in Bayes estimate framework as follows:

$$\phi_j^* = \arg\max_{\forall\{\phi_j^c\}} P(f_j^c \mid \phi_j^c, \delta)P(\phi_j^c) \qquad (5)$$

where ϕ_j^c is a planar surface model candidate generated for a local terrain; f_j^c is the observation when given ϕ_j^c and δ; $P\left(f_j^c \mid \phi_j^c, \delta\right)$ is the conditional probability density function of the observation f_j^c; $P(\phi_j^c)$ is the prior probability of the model ϕ_j^c. Thus, an optimal solution ϕ_j^* can be found as maximizing Eq. (5).

3. OVERALL STRATEGY

In this section, we discuss several important concepts used for implementing our terrain surface reconstruction algorithm; firstly, we define a criterion selected to differentiate the on- and off-terrain points and describe its role in the current framework; secondly, we explain how to measure the closeness between the plane surface model and its labelling observation used in Eq. (5); finally, we describe overall strategy to reconstruct real terrain surface as a set of piecewise planar surface models.

3.1 Plane Terrain Prior

Since it is assumed *a priori* that the underlying local area is flattened by a planar surface model, our criterion to differentiate on- and off- terrain points can be applied to the entire terrain surface model with the same meaning in such a way as to classify a LIDAR dataset into on- and off-terrain points when the underlying area is projected into a horizontal flat terrain.

To this end, we select a constant δ_h as the criterion, which is vertical height measured relative to a local terrain surface model ϕ_j. Once a local terrain surface is reconstructed by the planar surface model ϕ_j, this reconstructed terrain surface is *a priori* assumed as being "flat" and relative vertical heights of underlying LIDAR points are recomputed from ϕ_j. Then, the constant criterion δ_h straightforwardly assigns corresponding labels to underlying LIDAR points S_j located within ϕ_j; if a relative height of a point measured from ϕ_j is less than δ_h, an on-terrain label is assigned to this point; otherwise, an off-terrain one (see Figure 2). This labelling process using δ_h is universally applied to the entire LIDAR data regardless of terrain surface variances and thus, δ_h is independent of ϕ_j. Eq. (2) can be rewritten as follows:

$$f_j = \{f_i\}_{i=1}^N; \ \forall s_i \in S_j \ \ f_i = \mathrm{F}\left(s_i \mid \phi_j, \delta_h\right); \ f_i \in \{on, off\} \qquad (6)$$

where f_j is a set of labelling observations generated when ϕ_j is given. Once the model ϕ_j reconstructs a local terrain surface, it is required to determine whether this terrain reconstruction process would continue over the underlying area. If a condition to trigger the process is satisfied, the underlying terrain is fragmented even further in order to be made more flattened, and this process continues until its termination condition is satisfied.

The δ_h selected is used to provide a triggering and terminating condition for terrain fragmentation. As seen in Figure 2, assume that we have a set of LIDAR points S_j, and ϕ_j is used as a local plane terrain surface model. According to Eq. (3), on-terrain points populated by using δ_h must be satisfied with following condition; $\phi_j \mathbf{s}_j^{on} = 0$ where $\mathbf{s}_j^{on}$ is vector of on-terrain points belonging to S_j. If there exists any on-terrain point with which this conditioning property is not satisfied; $\phi_j \mathbf{s}_j^{on} \neq 0$, it indicates terrain surfaces having different slopes coexist within the underlying area and ϕ_j is not enough to make it flattened. Thus a terrain fragmentation process is triggered to seek more planar surface models to reconstruct underlying terrain surface as being plane.

We shall define a "buffer space" as one located between the terrain surface model ϕ_j and δ_h, which needs to be empty of any LIDAR point to make the terrain fragmentation process terminate (Figure 2). The emptiness of "buffer space" characterizes a plane terrain surface in a sense that when a local area is properly flattened by ϕ_j, there must be a discontinuity within the "buffer space", in which any LIDAR point cannot be located. Hence, both emptiness of "buffer space" and prior assumption of plane terrain surface for underlying area control trigger and terminate overall terrain surface reconstruction process in our research.
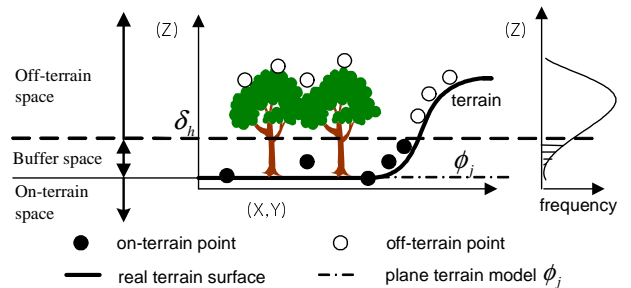
Figure 2. Illustration of a "buffer space" used to provide a triggering and terminating condition for the terrain fragmentation process.

3.2 Terrain Polarity Measurement

If the terrain fragmentation process is triggered, the remaining problem is to seek the "best fit" planar surface model to reconstruct underlying real terrain surface as being plane. To this end, it is necessary to discuss a criterion for this model selection problem. Let us define an intra-relationship of on-

terrain points as seen in Figure 3(a), in which two neighbouring on-terrain points are connected with each other, and then measure an angle difference θ_{on-on} between the terrain surface model ϕ_j and "on-on" paired observation. Similar to this, an inter-relationship of "on-off" paired observation can be also defined and its angle difference θ_{on-off} is measured from ϕ_j as seen in Figure 3(b).

In our research, these two different angle measurements are used to test the hypotheses of planar terrain surface models generated by assumption of the flat terrain. If a planar terrain surface model hypothesized correctly reconstructs real terrain surface as being "flat", on one hand, the slope angle of the model used reflects real terrain slope. On the other hand, two angles θ_{on-on} and θ_{on-off}, which are relatively measured from the planar terrain surface model, show the characteristics of plane terrain surface; i) θ_{on-on} gets closer to 0° since the labelling error that on-terrain points are misclassified as off-terrain, becomes smaller and thus, intra-relationships of on-terrain points follow the tendency of plane terrain slope; ii) θ_{on-off} gets closer to 90° in which off-terrain points show obvious discontinuity from plane terrain slope. These characteristics can be augmented when the underlying real terrain surface is more flattened by a hypothesized planar surface model; otherwise, the labelling error becomes larger and thus, it degenerates these characteristics of a plane terrain surface.

Based upon previous observations, we assume that a characteristic of plane terrain surface can be given by the observation of "bi-polarity", in which the smoothness and discontinuity polarity are defined as a distribution of θ_{on-on} of "on-on" paired observations and a distribution of θ_{on-off} of "on-off" ones respectively. Figure 3(c) shows a desirable distribution of plane terrain surface in terms of the terrain polarity measurement, in which two peaks of "bi-polarity" distribution appear close to 0° and 90° respectively when given ϕ_j correctly reconstructs the real terrain surface as being plane; otherwise, it shows a Gaussian distribution.
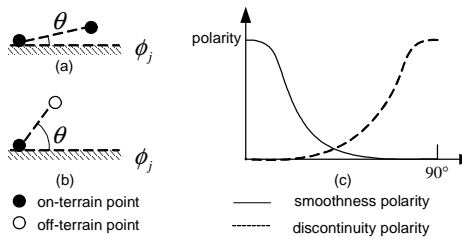
Figure 3. Illustration of terrain polarity measurement.

Hence, the terrain polarity measurement serves as a criterion for the selection of "best fitt" planar surface model out of the model candidates hypothesized; a surface model to show the strongest polarity, where two peaks get much closer to the polarity boundaries 0° and 90°, is selected as an optimized model solution. In our framework, this terrain polarity measurement is converted into the conditional probability density function used in Eq. (5) and finally described in the form of Minimum Description Length (MDL). This will be discussed in a later section.

3.3 Two-step Divide-and-Conquer Triangulation

Let us discuss how to determine the dimension k of the terrain surface model space ψ^* in Eq. (4). As discussed previously in Eq. (4), the determination of k is related the ability to find an on-terrain point out of a point cloud; k increases as on-terrain points are iteratively obtained. This recursive process terminates when any on-terrain point cannot be found, and results in a set of planar surface models $\{\phi_j^*\}_{j=1}^k$ satisfying Eq. (4).

We adopt the *divide-and-conquer* triangulation approach, in which the original problem domain is recursively decomposed into sub-problems and represented by means of a Delaunay Triangulation. This *divide-and-conquer* triangulation is implemented as two parts in our framework, namely downward and upward *divide-and-conquer* triangulation, depending on the criteria of triggering and terminating this process. In the downward process, the dimension k of the terrain surface model space ψ is initialized as 1, so that an initial terrain surface model is approximated with only one planar surface model; $\psi = \{\phi_j\}_{j=1}^k$, where $k=1$. Then, on-terrain points are recursively obtained by the use of pre-specified propositions of the terrain surface model so that the initialized ψ is fragmented into a number of planar surface models represented in a form of TIN. This terrain segmentation process continues until any negative LIDAR point located underneath the reconstructed terrain surface model cannot be found.

The upward *divide-and-conquer* triangulation is the core part of our terrain surface reconstruction technique, in which the afore-mentioned "plane terrain prior" and "terrain polarity measurement" are used. The process investigates the triggering condition for terrain fragmentation over all planar surface models generated by the downward *divide-and-conquer* triangulation. Once the terrain fragmentation process is triggered over a planar surface model ϕ_j, a number of tetrahedral models are hypothesized as planar surface models in a sense that three lateral facets of a tetrahedron are used as plane terrain surface model candidates. Then, distributions of terrain polarity are measured over all tetrahedral models. Thus, the most optimized tetrahedral model satisfying with the optimality criterion of Eq. (5) is selected and the on-terrain point newly found by this model contributes to refining ψ.

This process continues until the terminating condition for the terrain fragmentation process is found over the entire terrain surface model. The process of downward and upward divide-and-conquer triangulation will be discussed in detail in the following section.

4. TERRAIN SURFACE MODEL RECONSTRUCTION

Fig. 4 shows an overall process used for reconstructing the terrain surface model. In this section, we discuss the fore-mentioned overall strategy in more detail according to the blocks depicted in Fig 4.
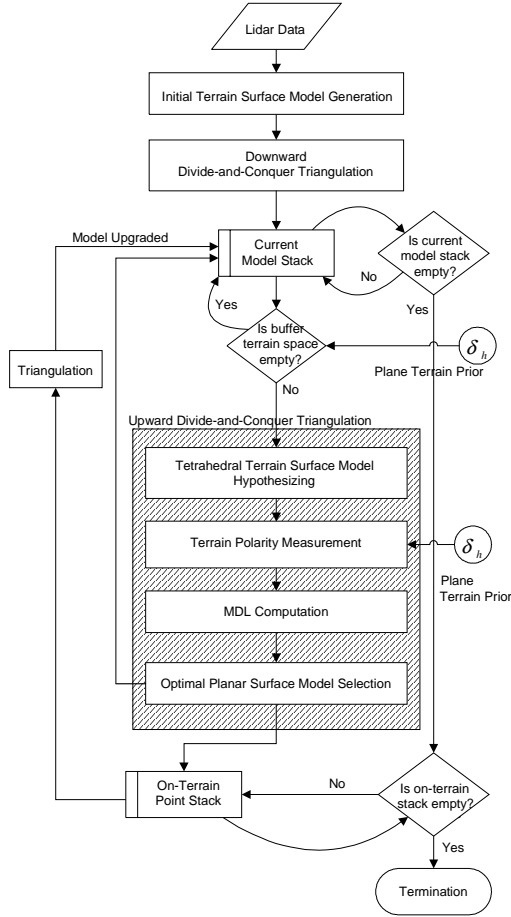
Figure 4. Overall strategy implemented in our terrain surface reconstruction algorithm.

4.1 Initial Terrain Surface Model Preparation

A terrain surface model ψ is initialized with a rectangle, which has four corner points assigned as on-terrain points. These corner points can be easily computed by the use of the domain information of the LIDAR dataset. First, a rectangle that covers the entire LIDAR points S is generated and the x and y coordinates of its four vertices are computed from the given domain information of S. A TIN is constructed using the entire S and the four vertices of the rectangle generated. Then, z values of neighbouring points connected to each corner point are averaged, and this value is assigned to the z values for the four vertices of the rectangle generated. These corner points are labelled as on-terrain points; hence the initial terrain surface model is prepared (see the top of Figure 5).

Since neighbouring points connected to the corner points are explicitly considered as on-terrain points for the computation of z values of the corner points, these may include errors. However, the size of a local terrain surface model reconstructed by the use of these corners gets smaller through our recursive *divide-and-conquer* triangulation process, hence its modelling error can be minimized.

4.2 Downward Divide-and-Conquer

We use two propositions for the downward *divide-and-conquer* triangulation process; 1) any point cannot be located underneath a reconstructed terrain surface model, and 2) if proposition 1 is

not valid within a local terrain surface model ϕ_j, a point with the maximum negative distance measured from ϕ_j is selected as the most reliable terrain point.

An initial terrain surface model is given as a rectangle $\{\phi_j\}_{j=1}^{k}$ where $k=1$. The first proposition is investigated over the individual ϕ_j. If any negative point located underneath a model ϕ_j is found, its distance is measured from ϕ_j and stored in a sequential data list. When this process is completed over ϕ_j, a point with the maximal negative distance is selected from the sequential list and assigned as an on-terrain point according to the second proposition. This investigation process to look for the negative points is made over the entire model space $\{\phi_j\}$.

Then, a TIN is constructed by these newly found on-terrain points and the ones used for a previous terrain model. Hence, the dimension k of the reconstructed terrain model increases. This downward *divide-and-conquer* triangulation process continues until no negative point is found within the entire model $\{\phi_j\}$ (see Figure 4 & 5).
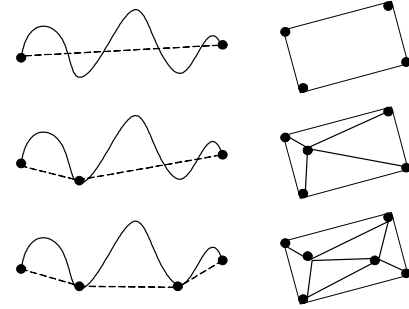
Figure 5. Illustration of the downward *divide-and-conquer* triangulation process.

4.3 Upward Divide-and-Conquer

A set of the planar terrain surface models $\{\phi_j\}$ reconstructed by the downward *divide-and-conquer* triangulation is stored in the form of TIN in the "current model stack", from which a model ϕ_j is selected. A set of member points S_j located within ϕ_j is obtained and its relative vertical heights measured from ϕ_j are computed. Then, a condition for terrain fragmentation mentioned in the previous section is investigated over ϕ_j when δ_h is given; if the buffer terrain space generated by δ_h is not empty, the upward *divide-and-conquer* triangulation is triggered; otherwise, this process does not continue for ϕ_j and the next model is selected from the "current model stack", over which the triggering condition for terrain fragmentation is reinvestigated (see Figure 4).

When the upward *divide-and-conquer* triangulation is triggered, a new on-terrain point is found through a series of processes, which will be discussed in the following sections and then this newly found on-terrain point is stored in the "on-terrain point stack" (see Figure 4). This process continues until all models stored in the "current model stack" are investigated. Then, if any new on-terrain point is found from the "on-terrain point stack", this is added up to the on-terrain points stored in the "current model stack". Using this new set of on-terrain points, the current terrain surface model is upgraded by the Delaunay

Triangulation. However, if no new on-terrain point can be found from the "on-terrain point stack" after the upward *divide-and-conquer* triangulation is completed over the entire current model space, our terrain reconstruction process is terminated (see Figure 4).

4.3.1 Observation Model

Once the upward *divide-and-conquer* triangulation process is triggered for certain areas reconstructed by a planar terrain surface model ϕ_j, the remaining problem is to look for "the most reliable" on-terrain point from LIDAR dataset S_j located over ϕ_j so that this local area is fragmented into more planar terrain surface models. To this end, a tetrahedron model T_j^i is adopted for terrain fragmentation of ϕ_j, in which the base triangle of T_j^i corresponds to ϕ_j and the remaining three lateral facets of T_j^i are hypothesized as planar surface models where i is the index of the tetrahedron model candidates generated over ϕ_j and k is the index of facets which comprise a tetrahedron model T_j^i (see Figure 6(a)).
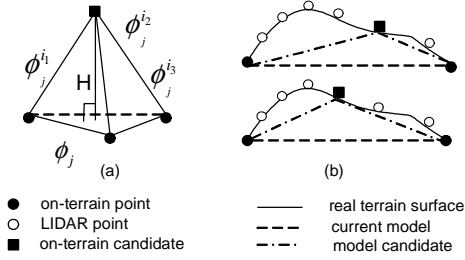
Figure. 6 Illustration of the generation of tetrahedron model candidates. (a) Tetrahedron model T_j^i, where H is the height T_j^i. (b) The generation of two different tetrahedron model candidates.

Since three vertices of ϕ_j are labelled as on-terrain points at the previous iteration step of our terrain reconstruction process, the remaining vertex of the tetrahedron T_j^i is used to hypothesize an on-terrain point out of S_j. Thus, a set of tetrahedron model candidates $\{T_j^i\}$ is generated, sharing its base triangle with ϕ_j and using each point of S_j as the remaining vertex of T_j^i (see Figure 6(b)). However, during the generation of $\{T_j^i\}$, T_j^i satisfying the following condition is rejected; $\forall k \in \{1,2,3\}$ $\phi_j^{i_k} \mathbf{s}_j^{i_k} < 0$, where $\phi_j^{i_k}$ is one of three lateral facets of T_j^i and $\mathbf{s}_j^{i_k}$ is vector of LIDAR dataset belonging to the model candidate $\phi_j^{i_k}$.

For simplifying mathematical notations, let us consider one of three lateral facets $\phi_j^{i_k}$ as ϕ. Suppose then LIDAR dataset S is located over ϕ as seen in Figure 7(a). Since the underlying area is hypothesized as a plane terrain surface by ϕ, the vertical height of each point of S is recomputed relative to ϕ so that z values of LIDAR points S, are projected into a flat horizontal

plane. Then, a set of labelling observations f for S is generated by Eq. (6) when δ_h is given (see Figure 7(b)).
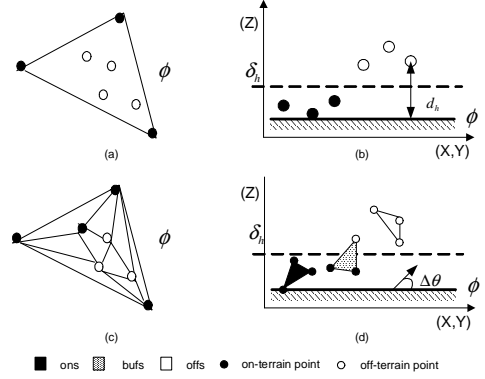
Figure. 7 Illustration of observation model used for the polarity measurement.

In order to make inter- and intra-relationships for on- and off-terrain points, a TIN is constructed over f as seen in Figure 6(c). Now, let us introduce a new observation variable γ_i for the terrain polarity measurement using this TIN. Suppose that we have a labelling function R which assigns a new labelling observation γ_i to each triangle Δ_i of TIN from a semantic label set {ons, bufs, offs} (see Figure 7(d)); a "ons" is assigned to Δ_i when all the three vertices of Δ_i are labelled as on-terrain points by Eq. (6); similarly to this, "bufs" is assigned when Δ_i is comprised of the mixture of on- and off-terrain points; otherwise, "offs" when all the vertices of Δ_i are labelled as off-terrain points. This labelling function R can be described as follows:

$$\gamma = \{\gamma_i\}_{i=1}^{N}; \ \forall s_i \in S_j \ \gamma_i = R(\Delta_i); \ \gamma_i \in \{ons, bufs, offs\} \tag{7}$$

$$R(\Delta_i) = \begin{cases} ons & if \ F(\{s_i, s_j, s_k\} \mid \phi, \delta_h) = \{on\} \\ bufs & if \ F(\{s_i, s_j, s_k\} \mid \phi, \delta_h) = \{on, off\} \\ offs & if \ F(\{s_i, s_j, s_k\} \mid \phi, \delta_h) = \{off\} \end{cases} \tag{8}$$

Where in Eq. (8), $\{s_i, s_j, s_k,\}$ are three vertices of Δ_i and F is the labelling function for a single LIDAR point. Now, we can measure the closeness between ϕ and γ in terms of terrain polarity measurement, in which $\Delta\theta$ serves as a parameter to determine a degree of the smoothness and discontinuity polarity depending on a label assigned to Δ_i. This $\Delta\theta$ is defined as follows:

$$\Delta\theta = \left| \theta_{\Delta_i} - \theta_\phi \right| \tag{9}$$

where $\Delta\theta$ is the angle difference between the slope of a triangle Δ_i and the one of a planar surface model ϕ, namely θ_{Δ_i} and θ_ϕ respectively.

4.3.2 Minimum Description Length Criterion

The *minimum description length* (MDL) criterion by Rissanen (1984) provides a generic method for comparing the optimality of different models fitted to particular observations (Cham, 1999). In our terrain surface reconstruction process, this MDL criterion is employed in order to determine an optimised model T_j^* out of the tetrahedron model candidates $\{T_j^i\}$ generated for ϕ_j. In Eq. (5), let us substitute the model candidate ϕ_j^c and its labelling observations f_j^c for a tetrahedron model T_j^i and its new observations of the terrain polarity γ_j^i respectively. For simplifying the notation, let us describe a tetrahedron model candidate as T_j and its set as $\{T_j\}$. Then, Eq. (5) can be reformulated as follows:

$$T^* = \arg\max_{\forall\{T_j\}} P(\gamma_j \mid T_j, \delta) P(T_j) \qquad (10)$$

where γ_j is a set of labelling observations measured for all the three lateral facets of T_j given, which is generated by Eq. (7) and (8).

According to the MDL framework, when we take the minus logarithm based 2 on both sides of Eq. (10), maximizing the *a posteriori* probability density function of Eq. (10) in order to select the optimized model, T^* can be converted into minimizing the total coding length of describing observations γ_j using model T_j as follows:

$$L^*(\gamma^*, T^*) = \min_{T_j \in \{T_j\}} \left[-\log_2 P(\gamma_j \mid T_j, \delta_h) + L(T_j) \right] \qquad (11)$$

where the first term of Eq. (11) is the description length to encode the closeness between the model T_j and its observations γ_j, that is a degree of the terrain polarity and the last term $L(T_j)$ specifies the description length of the parameters of the tetrahedron model T_j as its length increases, when the model complexity gets larger. Thus, the MDL optimality in Eq. (11) can be achieved when the terrain polarity of plane terrain surface is augmented most strongly and the model T_j used is the simplest one of the candidates $\{T_j\}$.

Li (1993) suggested that the description length of the entire observations γ_j can be efficiently encoded in the MDL framework, when given model T_j is divided into two parts, the inlier model part and the outlier part, i.e., $T_j = [T_j^{in} + T_j^{out}]$, here T_j^{in} is the inlier model fitted to the observations of "ons" and "bufs" generated by Eq. (8) and T_j^{out} is outlier part fitted to "offs" ones. Thus, given T_j, the total description length of γ_j is described as follows:

$$L(\gamma_j, T_j) = \sum_{\forall \gamma_i \in \gamma_j} \left[-\log_2 P(\gamma_i^{ons} \mid T_j, \delta_h) - \log_2 P(\gamma_i^{bufs} \mid T_j, \delta_h) \right]$$
$$+ L(T_j^{out}) + L(T_j^{in}) \qquad (12)$$

where γ_i is an observation generated by Eq. (7) and (8) when given T_j; γ_i^{ons} and γ_i^{bufs} are labelling observations generated depending on which label is assigned to γ_i by Eq. (8), that is "ons" or "bufs".

In Eq. (12), the first term and second terms indicate lengths of a degree of the smoothness and discontinuity of the terrain polarity respectively, which are differently measured depending on the label of γ_i. Thus, when $\Delta\theta_i$ is measured for γ_i according to Eq. (9), the conditional probability for the model T_j and an observation γ_i is given as follows:

$$P(\gamma_i \mid T_j, \delta_h) = \begin{cases} \dfrac{1}{1 + e^{+\alpha(\Delta\theta_i - \beta)}} & \text{if } R(\Delta_i) = ons \\ \dfrac{1}{1 + e^{-\alpha(\Delta\theta_i - \beta)}} & \text{if } R(\Delta_i) = bufs \end{cases} \qquad (13)$$

where α and β are the parameters for the sigmoidal function which generates a normalized probability density function; its minimum and maximum probability is restricted up to 0 and 1 respectively. In Eq (13), the probability is maximized when $\Delta\theta_i$ of "ons" observation describing an intra-relationship of on-terrain points is measured close to 0°. Similarly, when "bufs" one of inter-relationship between on- and off-terrain points is measured close to 90°, the probability is also maximized. In this case, their description lengths in Eq. (12) get shortened.

The last two terms in Eq. (12) are the description lengths for T_j^{out} and T_j^{in} respectively. $L(T_j^{out})$ is the description length of the number of outliers, that it $L(T_j^{out}) = -\log_2 N_{offs}$, which means that our objective function of Eq. (12) prefers a model which populates more off-terrain points when the strengths of the terrain polarity are comparable between model candidates.

Likewise, $L(T_j^{in})$ is the description length of a tetrahedron model used. Since the entire model candidates $\{T_j\}$ share the same base triangle, the only difference that can be characterized for an individual model is the size of volume of T_j, which is proportional to its height H_j. Thus, the description length to encode T_j^{in} is generated as follows: $L(T_j^{in}) = \log_2 H_j$, which means that when the optimized model T^* is selected, we expect that the terrain surface is reconstructed smoothly, rather than abruptly. Thus, the model having a smaller volume is preferred in Eq. (12).

When the upward *divide-and-conquer* triangulation is triggered over a local area, a set of the tetrahedron model candidates $\{T_j\}$ is generated and the description length of Eq. (12) is measured for all the three lateral facets of each T_j when δ_h is given. Finally, the model to have the minimum length of Eq. (12) is

selected as the optimized one, and its on-terrain points are stored in the "on-terrain point stack". This process continues until the upward *divide-and-conquer* triangulation is performed over all models stored in the "current model stack" (see Figure 4).

5. TEST DATA & RESULTS

We tested our suggested filtering technique with several different LIDAR dataset. Figure 8 (a) shows a test area located in east London with an Ikonos panchromatic imagery and the off-terrain points are extracted by our filtering algorithm from a LIDAR data, which was collected over the same area by the Optech 1020 sensor with 3 metre planimetric resolution (Figure 8 (b)). This area was selected since it contains a "good" mixture of different features and slopes, i.e., residential area, flat grass, knolls, forest and hills; it is suitable to validate how this filtering technique is continuously adaptive to terrain surface variations, especially for gently sloped terrain. Although overall the terrain is not flat and there are several gentle hills, our technique clearly extracted off-terrain points, while any points on the hills are not labelled as the off-terrain (see middle of the bottom in Figure 8 (b)).

Figure 9 (a) shows the Shrewsbury dataset in UK, which was acquired by the Optec 2033 sensor with 2 metre post spacing. As a result of the terrain surface reconstructed by our filter, Figure 9 (b) shows how the definition of terrain surface established in our filtering technique works in order to deal with terrain surface variations. In this example, one can see that our filtering algorithm recognized a railway embankment in the middle of figure as on-terrain points even though it has relatively steep slope (about 21°). This result is reasonable; if LIDAR points are located consecutively along the side of the railway embankment and one cannot observe the "emptiness" within the "buffer space" generated between the railway embankment and neighboring meadow, our terrain fragment process continues within that area and finally, the railway embankment is recognized as on-terrain points. For the same reason, but as a different result, a railway bridge located along the railway dam is detected as off-terrain points (see bottom of right side in Figure (b)).

Another result processed using the sub-area of the OEEPE data set of Vaihingen with the density of 0.18 points per square metre is shown in Figure 10. In this result, houses and a group of trees are removed, but geomorphologic features are well preserved after applying our filter.

Even though we used different test data set in terms of resolution and terrain type, we fixed our parameters as 1 metre for δ_h, 0.1 and 45 for α and β respectively in Eq. (13), but the results are robust for the parameter settings.

6. CONCLUSIONS AND FUTURE WORK

We have shown that by explicitly selecting the criterion to differentiate on-terrain points from off-terrain ones, a LIDAR filtering technique, which is continuously adaptive to terrain surface variations, may be developed. This method aims to recursively fragment the entire LIDAR data domain into a set of piecewise planar surface models in order to make underlying terrain slope variations regularized into homogeneous plane terrain. To this end, two characteristics of plane terrain surface are defined; i) there is an empty "buffer space" in which any

LIDAR point cannot be located over plane terrain, and ii) a "terrain polarity" made of a contextual information of on- and off-terrain points is augmented when it is measured from plane terrain. These characteristics are estimated over local areas reconstructed by a hypothesized planar surface model. By this means, our terrain reconstruction process is recursively triggered and an optimised planar model is selected. Since only one criterion for this method is explicitly required, our method can easily reflect the user requirement for the generic purpose of LIDAR filtering.

Although our algorithm is not optimized yet in terms of the computational speed, it demonstrated promising results of the terrain surface reconstructed using real LIDAR data. Based upon this result, our future work will seek to classify building and tree objects from the off-terrain points. This will enable an object to be classified as a building and it will serve as an efficient tool for building detection and model generation.

7. REFERECES

Axelsson, P., 2000. DEM generation from laser scanner data using adaptive TIN models. In: *The International Archives of the Photogrammetry, Remote Sensing and Spatial Information Sciences*, Annapolis, MD, Vol. XXXIII, Part B3/1, pp. 119-126.

Baillard, C. and Maitre, H., 1999. 3-D reconstruction of urban scenes from aerial stereo imagery: a focusing strategy. *Computer Vision and Image Understanding*, 76(3), pp.244-258.

Cham, T. J. and Cipolla, R., 1999. Automated B-spline curve representation incorporation MDL and error-minimizing control point insertion strategies. *IEEE Transactions on Pattern Analysis and Machine Intelligence*, 21(1), pp. 49-53.

Cobby, D. M., Mason, D. C. and Davenport I. J., 2001. Image processing of airborne scanning laser altimetry data for improved river flood modelling. *ISPRS Journal of Photogrammetry & Remote Sensing*, 56(2001), pp.121-138.

Flood, M., 2001. LIDAR activities and research priorities in the commercial sector. In: *The International Archives of the Photogrammetry, Remote Sensing and Spatial Information Sciences*, Annapolis, MD, Vol. XXXIV, Part 3/W4, pp. 3-7.

Li, M., 1993. Minimum description length based 2-D shape description. In: *Proceedings of 4th International Conference on Computer Vision*, Berlin, Germany, pp. 512-517.

Li, S. Z., 2001. *Markov Random Field Modeling in Image Analysis*. Springer-Verlag, Tokyo, pp. 3-8.

Pfeifer, N. and Kraus, K., 1998. Interpolation and filtering of laser scanner data – implementation and first results. In: *The International Archives of the Photogrammetry, Remote Sensing and Spatial Information Sciences*, Columbus, Vol. XXXII, Part 3/1, pp. 153-159.

Rissanen, J., 1984. Universal coding, information, prediction, and estimation. IEEE *Transaction of Information Theory*, 30(4), pp. 629-636.

Vosselman, G., 2000. Slope based filtering of laser altimetry data. In: *The International Archives of the Photogrammetry, Remote Sensing and Spatial Information Sciences*, Annapolis, MD, Vol. XXXIII, Part 3/2, pp. 935-942.

(a) Ikonos monocular imagery taken over the test area
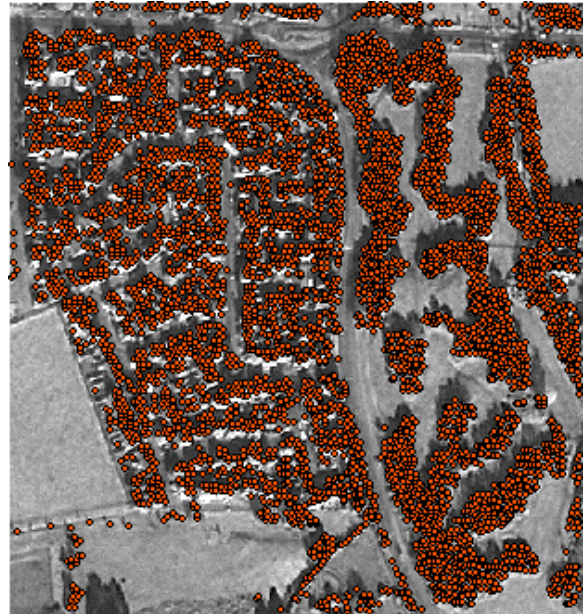
(b) Result of off-terrain points extracted by our method, which is shown as red dots

Figure. 8 Experimental results derived from real LIDAR dataset collected over a test area of east London. Lidar data supplied by and (C) Infoterra. Includes material which is (C) Space Imaging L.P.. IKONOS and LIDAR data for East London courtesy of Prof. J-P Muller and the BNSC-LINK RISKMAP project

(a) Interpolated original LIDAR data

(b) Result of the terrain surface reconstructed by our method

Figure. 9 Experimental results derived from real LIDAR dataset collected over a test area of Shrewsbury in UK LIDAR data courtesy of the Environment Agency of U.K.
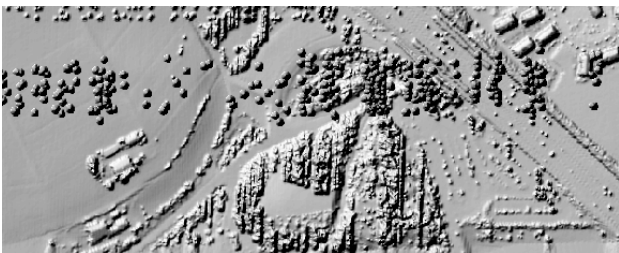
(a) Interpolated original LIDAR data

(b) Result of the terrain surface reconstructed by our method

Figure. 10 Experimental results derived from real LIDAR dataset collected over Vaihingen area. LIDAR data courtesy of the OEEPE working groups on LIDAR and IfSAR.